

# On pressure impulse of a laser-induced underwater shock wave

**Yoshiyuki Tagawa<sup>1†</sup>, Shota Yamamoto<sup>1</sup>, Keisuke Hayasaka<sup>1</sup> and Masaharu Kameda<sup>1</sup>**

<sup>1</sup>Department of Mechanical Systems Engineering, Tokyo University of Agriculture and Technology, Nakacho 2-24-16 Koganei, Tokyo 184-8588, Japan

(Received ?; revised ?; accepted ?. - To be entered by editorial office)

We experimentally examine a laser-induced underwater shock wave with a special attention to pressure impulse, the time integral of pressure evolution. Plasma formation, shock-wave expansion, and pressure in water are observed simultaneously using a combined measurement system that obtains high-resolution nanosecond-order image sequences. These detailed measurements reveal a non-spherically-symmetric distribution of pressure peak, which is inconsistent with a well-known spherical-shock model. In contrast, remarkably, pressure impulse is found to distribute symmetrically for a wide range of experimental parameters. The structure is determined to be a collection of multiple spherical shocks originated from elongated plasmas.

**Key words:**

---

## 1. Introduction

Underwater shock waves induced by illumination with a nanosecond laser pulse are utilized in various applications including low-invasive medical treatments (Razvi *et al.* 1996; Sofer *et al.* 2002; Lam *et al.* 2002; Sankin *et al.* 2005; Klaseboer *et al.* 2007; Lee & Doukas 1999; Kodama *et al.* 2000). The laser-induced shock wave triggers a sudden motion of a liquid as well as a free surface, which, for instance, results in generation of high-speed microjets applicable for needle-free injection devices (Menezes *et al.* 2009; Thoroddsen *et al.* 2009; Tagawa *et al.* 2012, 2013; Marston & Thoroddsen 2015).

For the sudden motion of the liquid, one of the most important quantities is pressure impulse (Batchelor 1967; Cooker & Peregrine 1995; Antkowiak *et al.* 2007). Its definition is given as:

$$P = \int pdt, \quad (1.1)$$

where  $p$  is pressure of the liquid and  $t$  is the elapsed time. Peters *et al.* (2013) numerically reproduced the high-speed microjet reported by Tagawa *et al.* (2012) and confirmed that the pressure impulse is the key quantity for the motion of the jet. Thus detailed investigation for the pressure impulse of the laser-induced shock wave is of great importance.

The shock wave has been often modeled as a *spherical shock*, which assumes a spherically-symmetric pressure distribution and spherical shape of the shock. However, some researchers have pointed out that the spherical-shock model is not applicable in certain

† Email address for correspondence: tagawayo@cc.tuat.ac.jp

cases (Buzukov *et al.* 1969; Sankin *et al.* 2008; Noack & Vogel 1998; Vogel *et al.* 1996a). Buzukov *et al.* (1969) reported that a non-spherically-symmetric bubble is observed with the series of compression waves. Sankin *et al.* (2008) measured pressure peaks for a shock at various positions and determined that the peak pressure at a point in the direction perpendicular to the laser beam is more than twice as high as that in the direction of the laser. Vogel *et al.* (1996a); Noack & Vogel (1998) reported that the shape of a shock wave is not spherical due to conical plasma formation. Despite these considerations, a common model for the pressure impulse of laser-induced shock waves has not been developed.

In this study, we report on experimental observations of a laser-induced shock wave with a special attention to pressure impulse. We also propose a new model of the shock wave to rationalize the observations. Such an observation is, however, challenging because each phenomenon involved in generating the shock occurs within a short time; illumination with a laser pulse first triggers the emergence of plasma in water, which leads to rapid expansion of a bubble and emission of a shock wave (Noack & Vogel 1999; Lauterborn *et al.* 2001). The time scale for plasma growth is in the order of nanoseconds and the shock velocity in water is approximately 1500 m/s. To the best of the authors' knowledge, plasma growth, the expansion process of the shock, and pressure in water have been *simultaneously* measured for the first time, using a combined measurement system, in which ultra-high-speed recording systems and pressure sensors are installed.

## 2. Experimental setup and method

Figure 1 shows the combined measurement system. An underwater shock wave is induced by a 532 nm, 6 ns laser pulse (Nd:YAG laser Nano S PIV, Litron Lasers) focused through an objective lens to a point inside a water-filled glass tank (100×100×450 mm). Experimental parameters are magnification of objective lens (5× [N.A. 0.1], 10× [N.A. 0.25], 20× [N.A. 0.25], MPLN series, Olympus) and laser energy (2.6 mJ, 6.9 mJ, 12.3 mJ). The combined measurement system consists of two hydrophones (Muller Platte-Gauge, Muller) and two ultra-high-speed cameras. One of the hydrophones is placed 5 mm away from the focal point of the laser in the direction of the laser beam ( $\theta = 0^\circ$  direction). The other hydrophone is at the same distance but in the direction perpendicular to the laser beam ( $\theta = 90^\circ$  direction). One of the cameras is an ultra-high-speed camera (Imacon 200, DRS Hadland) with up to  $200 \times 10^6$  fps (5 ns time interval) and a 1200×980 pixel array to record plasma formation. The other camera is another ultra-high-speed video camera (Kirana, Specialized Imaging) with up to  $5 \times 10^6$  fps and a 924×768 pixel array for imaging shadowgraph of shock-wave propagation. This camera is synchronized with a laser stroboscope that operates with a pulse width of 20 ns as a back illumination source (SI-LUX 640, Specialized Imaging), the repetition rate of which is also up to  $5 \times 10^6$  Hz. A digital delay generator (Model 575, BNC) is used to trigger the laser, the hydrophones, the cameras, and the stroboscope. Each measurement was repeated more than three times under the same experimental conditions.

## 3. Results and discussion

Figure 2 (in which  $t$  denotes the elapsed time from the start of illumination with the laser pulse) shows the measurement results obtained with the 10× objective lens. Figure 2(i) shows a snapshot of the plasma luminescence in an elongated area, the major axis of which is in the direction of the laser beam. The image sequence of the plasma (Figure 3) suggests that all parts of the plasma emit strong light within  $\pm 5$  ns. Within this short duration, plasma formation starts at the beam waist of the laser focus and a

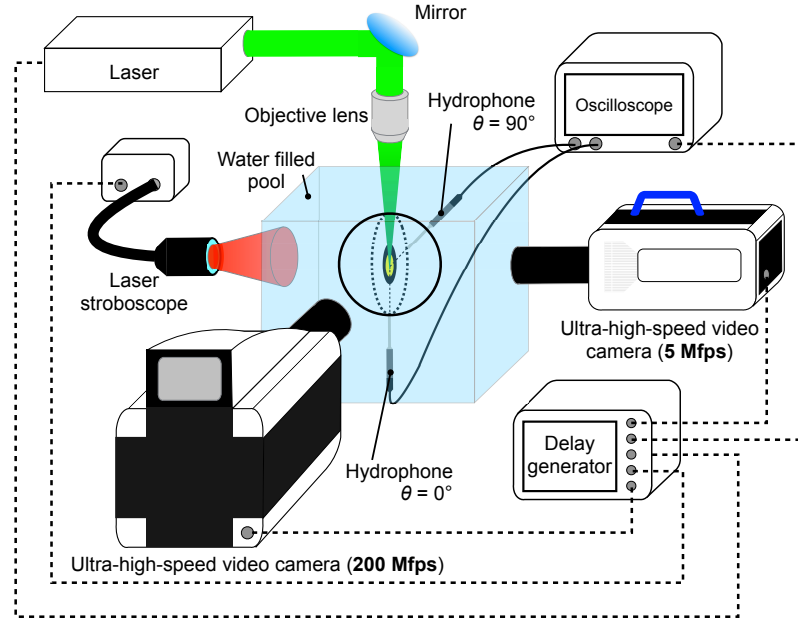


FIGURE 1. Measurement system consisting of two ultra-high speed cameras and two pressure sensors. An ultra-high speed video camera records laser-induced shock waves and bubbles at up to  $5 \times 10^6$  fps with a synchronized laser stroboscope. Plasma luminescence is captured by another ultra-high speed video camera at up to  $200 \times 10^6$  fps. Temporal pressure evolution is measured by two hydrophones. One hydrophone is arranged in the direction of the laser beam ( $\theta = 0^\circ$ ) at a stand-off distance of ca. 5 mm from the laser focal point, while the other hydrophone is at right angles to the hydrophone ( $\theta = 90^\circ$ ) at the same stand-off distance.

breakdown wave moves upstream towards the incoming laser pulse (Vogel *et al.* 1996*b*). A laser-induced bubble then emerges where the plasma was formed (Fig. 2(ii)) and its shape is also elongated in the direction of the laser beam. At  $t = 0.4 \mu\text{s}$ , non-single spherical shocks are observed. In contrast, at  $t = 2.4 \mu\text{s}$ , the shock could be regarded as a single spherical shock (see Fig. 2(iii)). However, enlarged images for  $\theta = 0^\circ$  and  $\theta = 90^\circ$  (Fig. 2(iii)) ( $\theta = 0^\circ$  and  $\theta = 90^\circ$ ) display a clear difference. Two shock waves for  $\theta = 0^\circ$  (Fig. 2(iii)) ( $\theta = 0^\circ$ ), which is different from the single shock wave for  $\theta = 90^\circ$  (Fig. 2(iii)) ( $\theta = 90^\circ$ ). Figure 2(iv) shows the temporal evolution of pressure measured with the two hydrophones placed at different positions. There are two peaks for  $\theta = 0^\circ$ , while there is a single large peak for  $\theta = 90^\circ$ , which is approximately 1.3 times higher than that for  $\theta = 0^\circ$ . Note that this dependence of the peak pressure on the angle  $\theta$  is the same as that reported by Sankin *et al.* (2008). For the  $5\times$  objective lens, this trend is much more pronounced: four plasma groups and four shock waves separated from each other are evident (see Fig. 4). Here, we compute the pressure impulse for  $\theta = 0^\circ$ ,  $P_0$ , and that for  $\theta = 90^\circ$ ,  $P_{90}$ . We calculate pressure impulse for  $t = 2.5$  to  $4.5 \mu\text{s}$ , during which time-lags of plasma formation ( $< 10 \text{ ns}$ ) is totally covered, i.e. the time-lags do not affect the results of pressure impulse. Both  $P_0$  and  $P_{90}$  for the shock obtained with  $10\times$  objective lens are shown in Fig. 2(iv) in the unit of  $\text{Pa}\cdot\text{s}$ .  $P_0$  is in reasonable agreement with  $P_{90}$ . Furthermore, pressure impulse and peak pressure for  $\theta = 0^\circ$  and  $90^\circ$  were examined for all the other experimental conditions. While peak pressure for  $\theta = 0^\circ$  and  $90^\circ$  differ significantly as shown in Fig 5(a), the  $P_0$  was in agreement with the corresponding  $P_{90}$  within the experimental uncertainty for a wide range of experimental

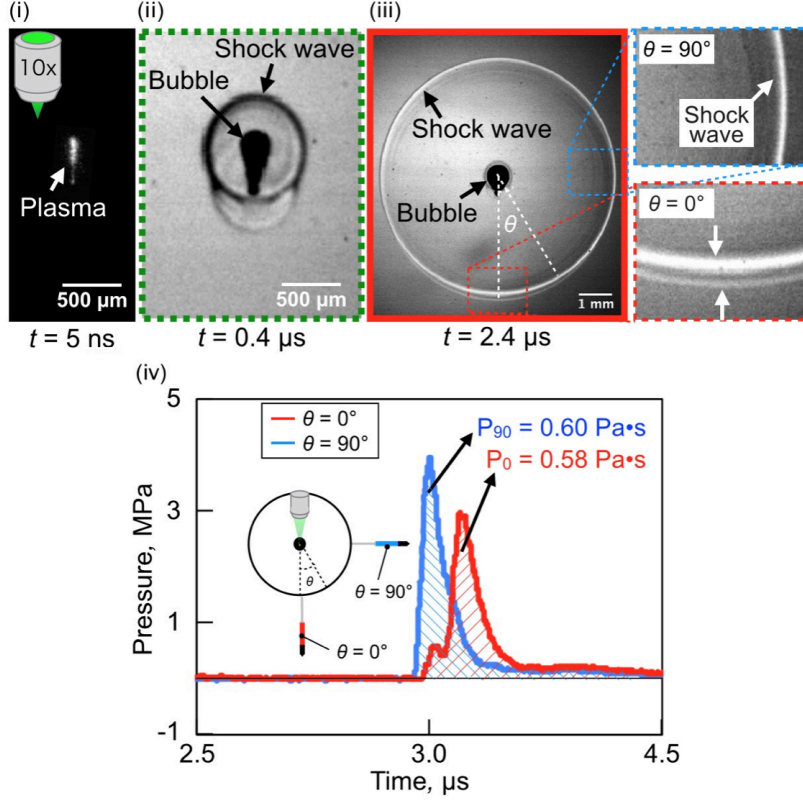


FIGURE 2. Measurement results for a laser-induced underwater shock wave obtained with a  $10\times$  objective lens. (i) Plasma luminescence at  $t = 5 \text{ ns}$  after the laser is fired. The image is captured by an ultra-high-speed video camera at 200 Mfps. (ii) Shock waves and bubbles at  $t = 0.4 \mu\text{s}$  imaged with an ultra-high speed video camera at 5 Mfps. (iii) Shock waves at  $t = 2.4 \mu\text{s}$  measured with an ultra-high-speed video camera at 5 Mfps. Enlarged images for the areas of  $\theta = 0^\circ$  and  $\theta = 90^\circ$  are also presented. (iv) Shock pressure measured by the two hydrophones arranged at  $\theta = 0^\circ$  (red line) and  $\theta = 90^\circ$  (blue line) with respect to the laser direction. Integrations for the pressure with respect to the elapsed time indicate pressure impulses.

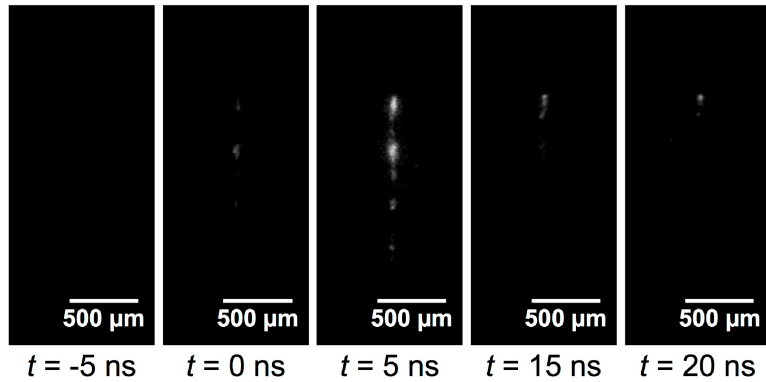


FIGURE 3. Temporal evolution of laser-induced plasmas obtained from ultra-high-speed video camera for the input energy of 6.9 mJ and 5x objective lens.

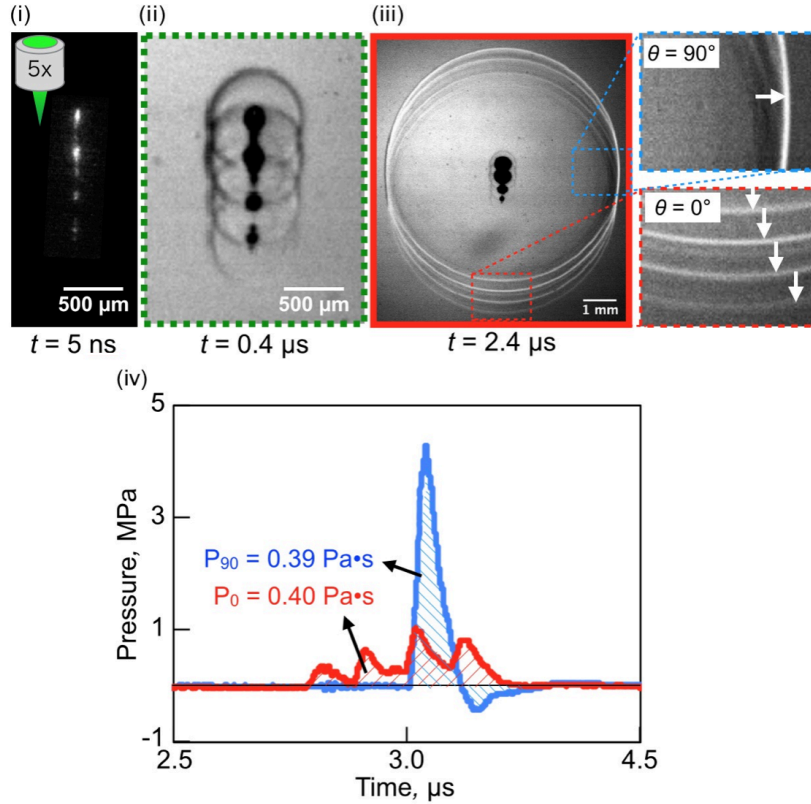


FIGURE 4. Measurement results for a laser-induced underwater shock wave obtained with a  $5\times$  objective lens. Captions for (i)-(iv) are the same as those in Fig. 4

parameters (Fig 5(b)). Note that the order of pressure impulse in this study is the same order of the practical use for drug delivery for cytoplasmic molecules (Kodama *et al.* 2000) and generation of microjets (Tagawa *et al.* 2012, 2013).

Based on the aforementioned results, we here propose a model for the structure of the laser-induced shock wave: The shock has a multiple structure that consists of multiple spherical shock waves as depicted schematically in Fig. 6. We assume that each spherical shock wave originates from the corresponding plasma formation. In addition, since the shock wave behaves acoustically with low pressure ( $\lesssim 100 \text{ MPa}$  (Vogel *et al.* 1996a)), we could apply the *superposition principle*: the net pressure that is produced by two or more shock waves reaching the same point is the sum of the pressure induced by the individual shock waves. A phenomenon that is analogous to this may be the surface wave observed after one or several stones are thrown into a quiescent pond (the so-called Huygens–Fresnel principle).

For both the  $10\times$  and  $5\times$  objective lens, this model rationalizes the observations of both pressure peaks and pressure impulse: several peaks for  $\theta = 0^\circ$  and the single large peak for  $\theta = 90^\circ$  while pressure impulse for  $\theta = 0^\circ$  matches pressure impulse for  $\theta = 90^\circ$ . Results for a wide range of experimental parameters (Fig 5) may indicate the universality of the multiple structure model. Note that this scenario includes the well-known spherical-shock model. It should be emphasized that, as observed with the  $10\times$  objective lens (Fig. 2), even if just a single plasma or a bubble is observed, the origin of the *elongated* plasma and bubble is expected to be multiple spots of plasma, which leads

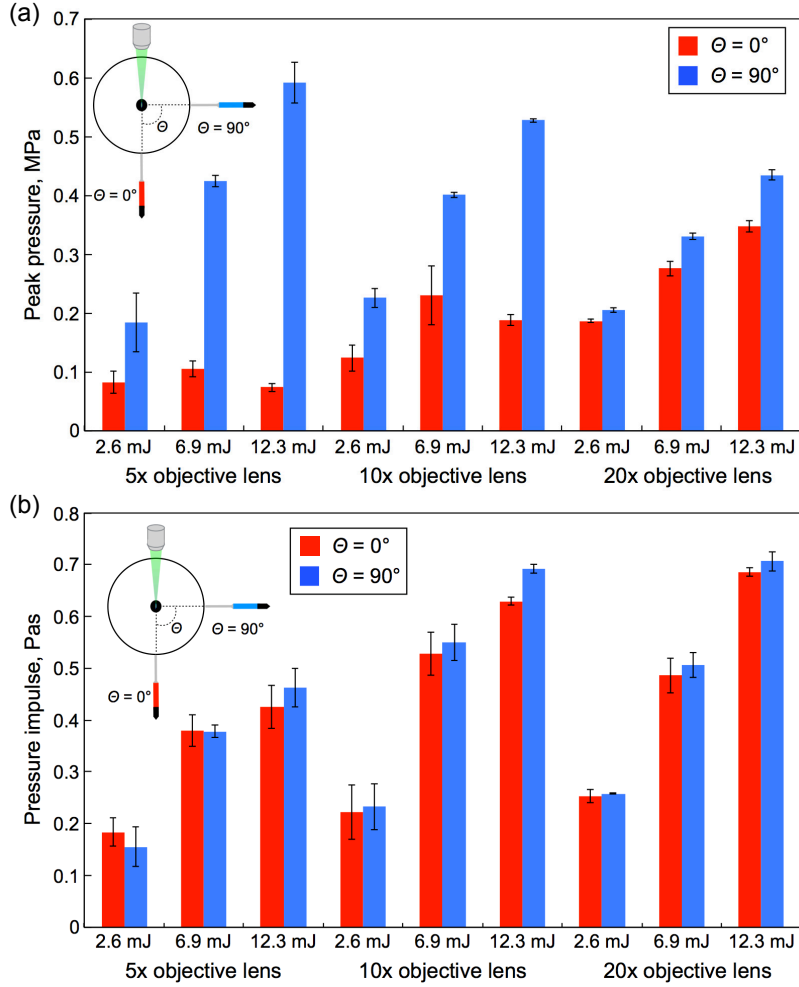


FIGURE 5. (a) *Peak pressure* of a laser-induced underwater shock wave measured at  $\theta = 0^\circ$  and  $\theta = 90^\circ$  for all the experimental conditions. Each presented value is a mean for three measurements and its error bar shows the standard deviation. (b) *Pressure impulse* of a laser-induced shock wave measured at  $\theta = 0^\circ$  and  $\theta = 90^\circ$  for all the experimental conditions.

to the emergence of a multiple spherical shocks, resulting in a notable angular variation of shock pressure. This model for the multiple shock structure could possibly rationalize the results reported in previous research. For instance, Sankin *et al.* (2008) reported that a laser-induced shock wave emitted from an elongated plasma has an angular variation of pressure distribution. Although the shape of the shock wave appears to be spherical, the elongated plasma shape may cause a multiple-structure of the shock, as observed in the present experiments (see Fig. 2), which would lead to a non-spherically-symmetric pressure peak of the shock.

Here, attention is given to plasma formation, which is the origin of the multiple shock structure. Figure 7 shows the plasma luminescence under all the experimental conditions. The multiple plasma formation is dependent on the spherical aberrations of the focusing optics, liquid impurities and the input laser energy (Vogel *et al.* 1996*a,b*; Nahen & Vogel 1996). Plasma is generated where the energy density is locally enhanced (Vogel *et al.*

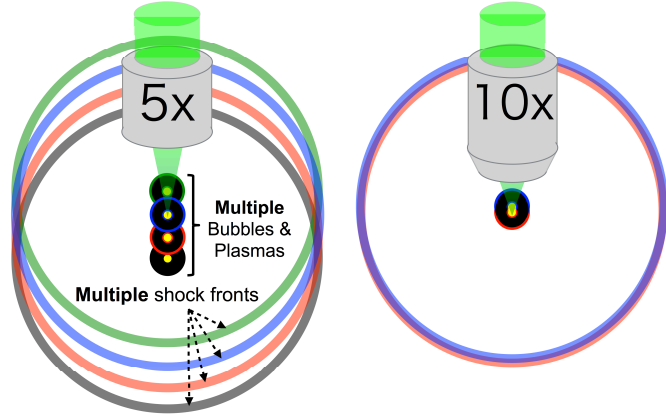


FIGURE 6. Schematic of a multiple structure model for a laser-induced underwater shock wave. Multiple plasmas emit multiple bubbles and spherical shock waves. The shock pressure at a certain point is the sum of spherical shock pressures that reach the same point.

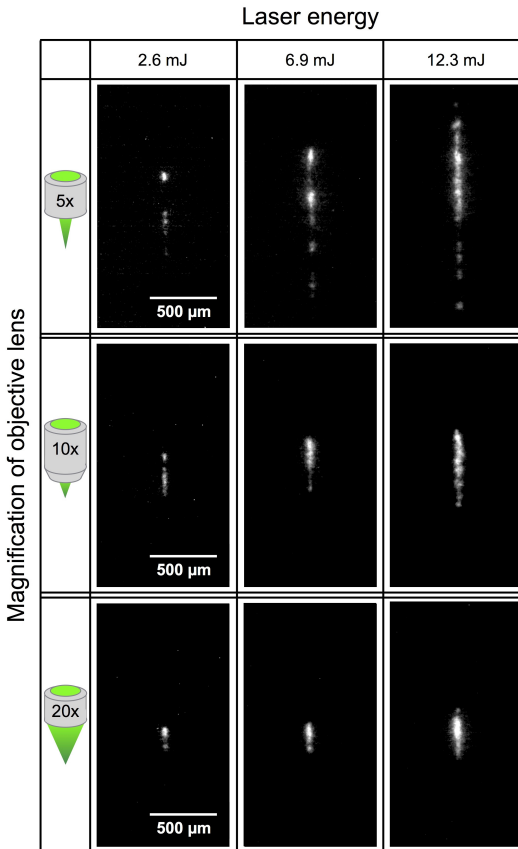


FIGURE 7. Plasma formation under all experimental conditions (Magnification of objective lens: 5×, 10×, 20×. Laser energy: 2.6, 6.9, and 12.3 mJ). The plasma shape is the most elongated with an input energy of 12.3 mJ and the 5× objective lens, whereas it is rather spherical with an input energy of 2.6 mJ and the 20× objective lens.

2005). As the input laser energy is increased, the region of plasma generation is enlarged more in the direction of the laser pulse beam, due to extension of the high energy density region. In the case of the  $5\times$  objective lens, the region of plasma generation is enlarged in the direction of the laser pulse beam, due to the small convergence angle (the maximum angle of the input laser beam to the optical axis). The regions of plasma generation with the  $10\times$  and  $20\times$  objective lens are smaller than that with the  $5\times$  objective lens because the convergence angles for the  $10\times$  and  $20\times$  objective lens are larger than that for the  $5\times$  objective lens.

#### 4. Conclusion and Outlook

In order to investigate a laser-induced shock wave with focusing on pressure impulse, we constructed a measurement system consisting of a combination of ultra-high-speed cameras and pressure sensors. Shock pressure was measured with two hydrophones arranged at  $\theta = 0^\circ$  and  $\theta = 90^\circ$  with respect to the laser direction, and plasma formation and shock wave expansion were simultaneously observed using two ultra-high-speed video cameras. The most important finding in this paper is that the distribution of pressure impulse of a shock wave is spherically symmetric for a wide range of experimental parameters even when the distribution of peak pressure is non-spherically-symmetric. We proposed a multiple structure model for the laser-induced shock wave: The laser-induced shock wave is a collection of spherical shock waves emitted from the bright spots inside the area of plasma luminescence. The multiple structure is dependent on the plasma shape generated by illumination with the laser pulse.

As an outlook, it should be noted again that the multiple shock structure ensures the same pressure impulse in all directions. This feature may provide high degrees of freedom for the design of needle-free injection devices using high-speed microjets. By changing the plasma shape with control parameters (magnification of the objective lens or the input laser energy), the anisotropy of the shock pressure could be controlled, which might be applicable to a variety of advanced techniques. Future numerical simulation based on the multiple-structure model is expected to provide additional support for this model.

#### Acknowledgments

The authors thank Shu Takagi and Yoichiro Matsumoto for the use of the Imacon 200 ultra-high-speed camera. This work was supported by Kakenhi Grant-in-Aid (No. 26709007) from the Japan Society for the Promotion of Science (JSPS).

#### REFERENCES

ANTKOWIAK, A., BREMOND, N., LE DIZÈS, S. & VILLERMAUX, E. 2007 Short-term dynamics of a density interface following an impact. *J. Fluid Mech.* **577**, 241–250.

BATCHELOR, G. K. 1967 *An Introduction to Fluid Dynamics*. Cambridge University Press.

BUZUKOV, A. A., POPOV, Y. A. & TESLENKO, V. S. 1969 Experimental study of explosion caused by focusing monopulse laser radiation in water. *J. Appl. Mech. Tech. Phys.* **10** (5), 701–708.

COOKER, M. J. & PEREGRINE, D. H. 1995 Pressure-impulse theory for liquid impact problems. *J. Fluid Mech.* **297**, 193–214.

KLASEBOER, E., FONG, S. W., TURANGAN, C. K., KHOO, B. C., SZERI, A. J., CALVISI, M. L., SANKIN, G. N. & ZHONG, P. 2007 Interaction of lithotripter shockwaves with single inertial cavitation bubbles. *J. Fluid Mech.* **593**, 33–56.

KODAMA, T., HAMBLIN, M. R. & DOUKAS, A. G. 2000 Cytoplasmic molecular delivery with shock waves: importance of impulse. *Biophys. J.* **79** (4), 1821–1832.

LAM, J. S., GREENE, T. D. & GUPTA, M. 2002 Treatment of proximal ureteral calculi: Holmium:yag laser ureterolithotripsy versus extracorporeal shock wave lithotripsy. *J. Urol.* **167** (5), 1972 – 1976.

LAUTERBORN, W., KURZ, T., SCHENKE, C., LINDAU, O. & WOLFRUM, B. 2001 Laser-induced bubbles in cavitation research. *IUTAM Symp. Free Surface Flows, Fluid Mechanics and Its Applications* **62**, 169–176.

LEE, S. & DOUKAS, A. G. 1999 Laser-generated stress waves and their effects on the cell membrane. *IEEE J. Selected Topics in Quantum Electronics* **5** (4), 997–1003.

MARSTON, J. O. & THORODDSEN, S. T. 2015 Laser-induced micro-jetting from armored droplets. *Exp. Fluids* **56** (7), 1–10.

MENEZES, V., KUMAR, S. & TAKAYAMA, K. 2009 Shock wave driven liquid microjets for drug delivery. *J. Appl. Phys.* **106** (8), 086102.

NAHEN, K. & VOGEL, A. 1996 Plasma formation in water by picosecond and nanosecond nd: Yag laser pulses. ii. transmission, scattering, and reflection. *IEEE J. Selected Topics in Quantum Electronics* **2** (4), 861–871.

NOACK, J. & VOGEL, A. 1998 Single-shot spatially resolved characterization of laser-induced shock waves in water. *Appl. Opt.* **37** (19), 4092–4099.

NOACK, J. & VOGEL, A. 1999 Laser-induced plasma formation in water at nanosecond to femtosecond time scales: calculation of thresholds, absorption coefficients, and energy density. *IEEE J. Quantum Electronics* **35** (8).

PETERS, I.R., TAGAWA, Y., OUDALOV, N., SUN, C., PROSPERETTI, A., LOHSE, D. & VAN DER MEER, D. 2013 Highly focused supersonic microjets: numerical simulations. *J. Fluid Mech.* **719**, 587–615.

RAZVI, H. A., DENSTEDT, J. D., CHUN, S. S. & SALES, J. L. 1996 Intracorporeal lithotripsy with the holmium:yag laser. *J. Urol.* **156** (3), 912 – 914.

SANKIN, G., SIMMONS, W., ZHU, S. & ZHONG, P. 2005 Shock wave interaction with laser-generated single bubbles. *Phys. Rev. Lett.* **95** (3), 034501.

SANKIN, G. N., ZHOU, Y. & ZHONG, P. 2008 Focusing of shock waves induced by optical breakdown in water. *J. Acoust. Soc. Am.* **123** (6), 4071–4081.

SOFER, M., WATTERSON, J., WOLLIN, T., NOTT, L., RAZVI, H. & DENSTEDT, J. 2002 Holmium: Yag laser lithotripsy for upper urinary tract calculi in 598 patients. *J. Urol.* **167** (1), 31–34.

TAGAWA, Y., OUDALOV, N., GHALBZOURI, E.A., SUN, C. & LOHSE, D. 2013 Needle-free injection into skin and soft matter with highly focused microjets. *Lab Chip* **13** (7), 1357–1363.

TAGAWA, Y., OUDALOV, N., VISSER, C. W., PETERS, I. R., VAN DER MEER, D., SUN, C., PROSPERETTI, A. & LOHSE, D. 2012 Highly focused supersonic microjets. *Phys. Rev. X* **2** (3), 031002.

THORODDSEN, S. T., TAKEHARA, K., ETOH, T. G. & OHL, C. D. 2009 Spray and microjets produced by focusing a laser pulse into a hemispherical drop. *Phys. Fluids* **21** (11), 112101.

VOGEL, A., BUSCH, S. & PARLITZ, U. 1996a Shock wave emission and cavitation bubble generation by picosecond and nanosecond optical breakdown in water. *J. Acoust. Soc. Am.* **100** (1), 148–165.

VOGEL, A., NAHEN, K., THEISEN, D. & NOACK, J. 1996b Plasma formation in water by picosecond and nanosecond nd: Yag laser pulses. i. optical breakdown at threshold and superthreshold irradiance. *IEEE J. Selected Topics in Quantum Electronics* **2** (4), 847–860.

VOGEL, A., NOACK, J., HÜTTMAN, G. & PALTAUF, G. 2005 Mechanisms of femtosecond laser nanosurgery of cells and tissues. *Appl. Phys. B* **81** (8), 1015–1047.